Where is the Non-Linear Rock Mechanics in the Linear Geomechanics of Gas Shales?

Nick R. Barton
NB&A, Oslo, Norway
nickrbarton@hotmail.com

Abstract: Gas-shales usually produce from several kilometers depth, with fracing-stimulation, propping, and subsequent registration of desirable 'clouds' of microseismic activity in the surrounding rock mass. This is presumed to be the initiation of shearing on natural fractures. Further shear may be aseismic when cohesive bonds have already been broken. The shale matrix which must have at least some porosity, is weaker than is typical for basement rocks. The potential pore pressure reduction of tens of MPa during the early life of the fields, a life which is very short according to some operators, may therefore be a significant proportion of the strength of the matrix. Inevitable non-linear rock strength behaviour for the matrix should not then be ignored. Significant moduli are also required for good production. It seems unrealistic to utilize a linear Mohr-Coulomb strength criterion as so frequently seen in oil industry geomechanics. The joints or natural fractures in the shales, which are presumed to be so important for production towards the inner propped region closer to the horizontal well section, will have producing fracture sets with different roughness and aperture. How many of them are planar enough to follow the linear Mohr-Coulomb behaviour always shown, where only a traditional 'Byerlee friction coefficient' is used? Where is the expected non-linear rock mechanics in the multi-discipline teams doing geomechanics? It has not yet been seen in numerous workshops, nor in oil industry courses on both sides of the Atlantic.

Key words: Shale gas, non-linear, shear strength, fractures, dilation.

1 Introduction

It has been known for many decades that the mechanical behaviour of fractures (the naturally occurring joint sets in a rock mass) is in general non-linear. The non-linearity is largely due to fracture roughness. (Barton, 1973, 2014a). In the case of intact rock, non-linear shear strength envelopes would be the result of large changes of effective stress caused by gas production. Non-linearity with respect to the jointing applies to the favourable shear strength-dilation-permeability coupling, which starts pre-peak, before Byerlee (friction coefficient based) strength is reached. The latter simplification for frictional strength from Stanford University, adopted by the geomechanics teams of many oil companies, misses the finess of pre-peak and post-peak dilatant shear strength. Non-linearity applies to the dilation accompanying shear, and especially applies to the less desirable stress-closure-permeability coupling of a stress-sensitive reservoir. Non-linear coupled-process (MH) modelling, partly based on the joint- or fracture-roughness coefficient (JRC), has been applied in rock mechanics (and reservoir compaction modelling) for more than 30 years, in discrete fracture codes like UDEC-BB, usually coupled with a joint wall strength parameter JCS.

The joint or fracture roughness JRC, also applies to the conversion from the hydraulically interpreted theoretical smooth-wall apertures (e) to the larger and non-planar-non-smooth-wall physical apertures (E), through which the gas (or oil) actually has to flow to the wells, in the case of gas shales or naturally fractured reservoirs. Simple index tests for acquiring JRC and JCS for the different fracture sets can be applied on fractures recovered in occasional and inevitably expensive core, and can also be estimated when mapping (or drone-photographing) fractured pavement analogues.

The conversion of a highly impermeable medium like shale into numerous gas-producing 'pay zones', using principal-stress steered, stress-and-structure oriented hydraulic fracturing, is a remarkable achievement. So remarkable

in fact that shear mobilization of natural fractures has also to be invoked to explain both the continued though declining production and the sources of larger 'radius' microseismic activity well beyond the assumed ellipsoidally-shaped tensile-fractured and sand-propped 'central' zones. The microseismic activity is believed to be the remote-sensing sign of shearing *initiation* of a large number of the natural fractures, needed for matrix drainage. The assumed shearing, and the resulting gas drainage, cannot occur in the case of gas-shales unless the shale is of high enough modulus to sustain the shear induced dilation, which results in a coupling with enhanced fracture permeability.

The pre-peak mobilization of roughness and permeability due to pre-peak dilation, combined with low in situ shear stiffness due to block-size related scale effects, is part of the rock mechanics reality behind critically stressed fractures. For reasons unknown, the expected non-linearity for both matrix and fractures is simplified as linear Mohr Coulomb events in petroleum geomechanics. In reality a more sophisticated and more favourable series of coupled processes are likely to be involved.

2 Moduli and Non-linear matrix strength

It is important to note from the review of King, 2010, that only shales with relatively high static deformation moduli will be good candidates for gas production. Non-prospective shales, as shown in Figure 1 in red, apparently have too low moduli e.g. 2-20 GPa to sustain productive propped-fractures and sheared-fractures. Values of 20 to 65 GPa – i.e. very 'rock-like' values, are apparently needed. In view of the fact that the strengths of shales are nevertheless limited in relation to hard crystalline rocks and in relation to hard carbonaceous rocks, it is appropriate to suggest that there is a strong likelihood that shales will reach the brittle-ductile transition and even *critical state*, as represented in Figure 2. This is because the perhaps 40 to 60 MPa (?) increase of effective stress caused by gas (or oil) production will represent a significant excursion of stress in relation to the limited strength. This is especially the case for porous carbonates such as chalk.

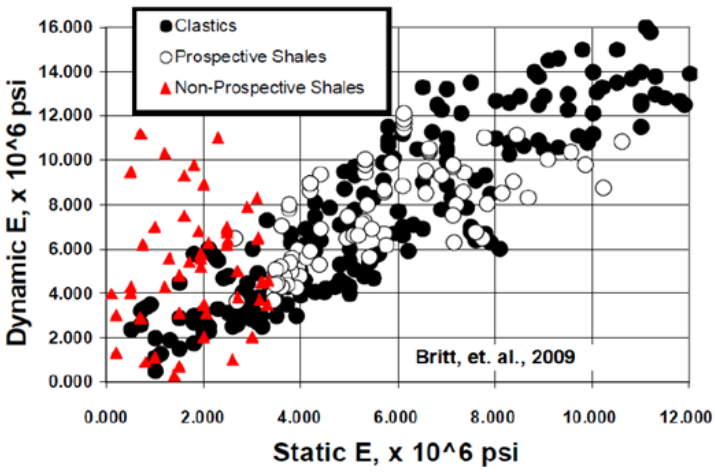

Figure 1 Correlation of Young's modulus between static tests on cores, and dynamic logs. The prospective gas producing shales group with the tight sandstone clastics, while the non-productive shales have a low static modulus and scattered dynamic modulus (King, 2010 from Britt et al. 2009).

Obviously the strengths of shales are limited in relation to hard carbonaceous rocks. Furthermore, effective stress levels are likely to increase by many 10's of MPa during production, which is unusually short-lived. It is appropriate to suggest the strong likelihood that shales will reach the brittle-ductile transition and even *critical state*, first of all at highly-stressed contacting asperities.

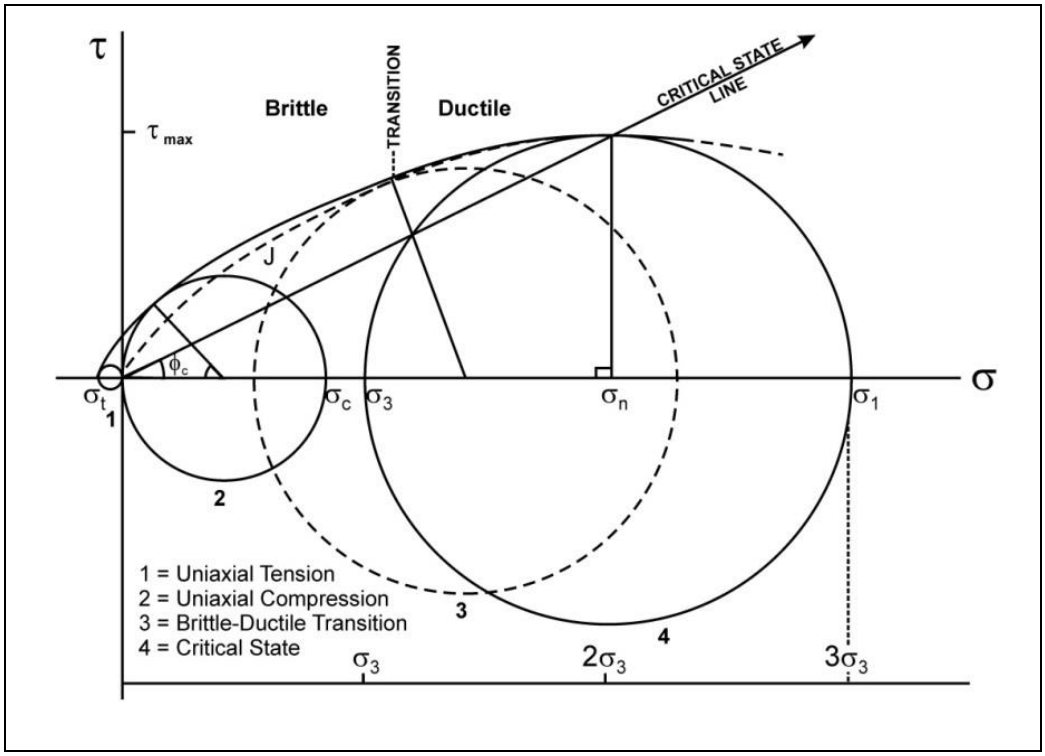

Figure 2 The critical state concept recently used by Singh et al. 2011, to derive the equations giving the correct deviation from the so frequently used linear Mohr-Coulomb assumption. Barton, 1976.

According to the studies of Singh et al., 2011, the majority of rock types have $\sigma_{3\ (critical)} \approx \sigma_c$. In other words Mohr circles #2 and #4 are touching or nearly touching, as illustrated in Figure 2. There is reason to believe that this non-linearity will be especially relevant in weaker (more clay-bearing) shales, as effective stresses increase during production. A few triaxial tests at low confinement give the complete curved envelope. This is not the case with other strength criteria. Tests are needed at many different confining pressures when less correctly curved strength criteria are used.

Because some of the producing gas-shales are significantly weaker than the USA's favoured Barnett shale, it is likely that effective confining stress levels will rise during production to levels exceeding, in some cases, their $\sigma_{3\ (critical)} \approx \sigma_c$ values. These near-critical effective confining stress levels will actually be reached first on the contacting (stress-transferring) 'asperities' which in the case of quite planar sheared fracture surfaces, will tend to be significant 'islands' of contact. It is likely to be the cumulative closure of these which will compromise continued production, until re-fracking near-by, and repeating the cycle of fracturing-propping-shear stimulating-draining.

3 The role of fracture deformation

The integration of natural joints or fracture sets in the production of shale gas requires both belief in and confirmation, that the clouds of microseismic events detected well outside the frac-simulated and sand-propped region (which is too small in volume to supply sufficient gas), actually signifies the mobilization of joints or fractures in shear. Some distance away from the high-volume, high- pressure fracking fluid (and sand-propped) region, conditions may exist (and need to exist), for fracture-shearing stimulation. This must occur beyond where slick-water is still invading the formation, and well beyond the sand-propped region. Otherwise insufficient volume is drained.

Figure 3 The relative planarity of fractures in shale seen in a pavement outcrop, from Han, 2011 and in a Kimmeridge Bay cliff outcrop of shale source-rock, from Barton, 2014b.

Quite planar examples of natural fractures are illustrated in Figure 3. The indirect stimulation of such natural fractures in shear, appears to be the key to sustained production from gas-shale reservoirs. Some incidences of shearing, which could also apply within the complex zone of propped hydraulic fractures, are illustrated in Figure 4. It is necessary to increase the surface area of shear-stimulated fracturing, so that gas can leave the matrix because of greatly increased permeability.

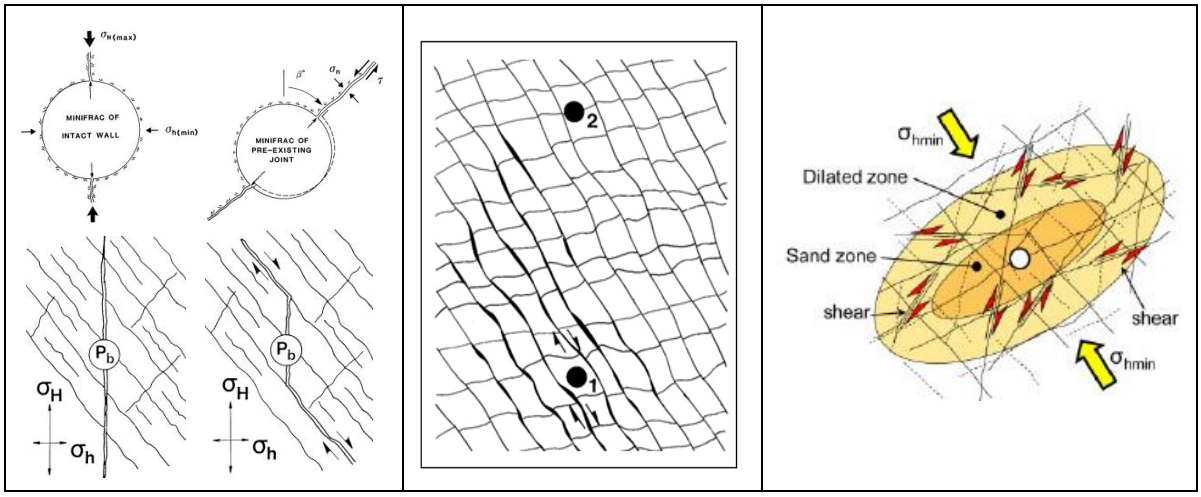

Figure 4 Alternative scenarios involving fracture shearing from minifrac (and fracking), from geothermal energy 'fracture-capture' and from gas shale stimulation. From Barton, 1981, Barton, 1986 and Dusseault, 2013. The right-hand figure is specific to gas-shale stimulation, and represents the assumption that shearing of fractures outside the 'central' sand-propped zone is the source of microseismic activity, and the key to production from 'impermeable' gas-shales.

There appears to be concern in some parts of the shale-gas industry about the quite rapid decline in pressure, and therefore the quite rapid decline in production. Many tens of MPa can be lost during for instance 250 days of (perhaps) too rapid production. The ability to shear natural fractures beyond the peripheries of the ellipsoidally-propped

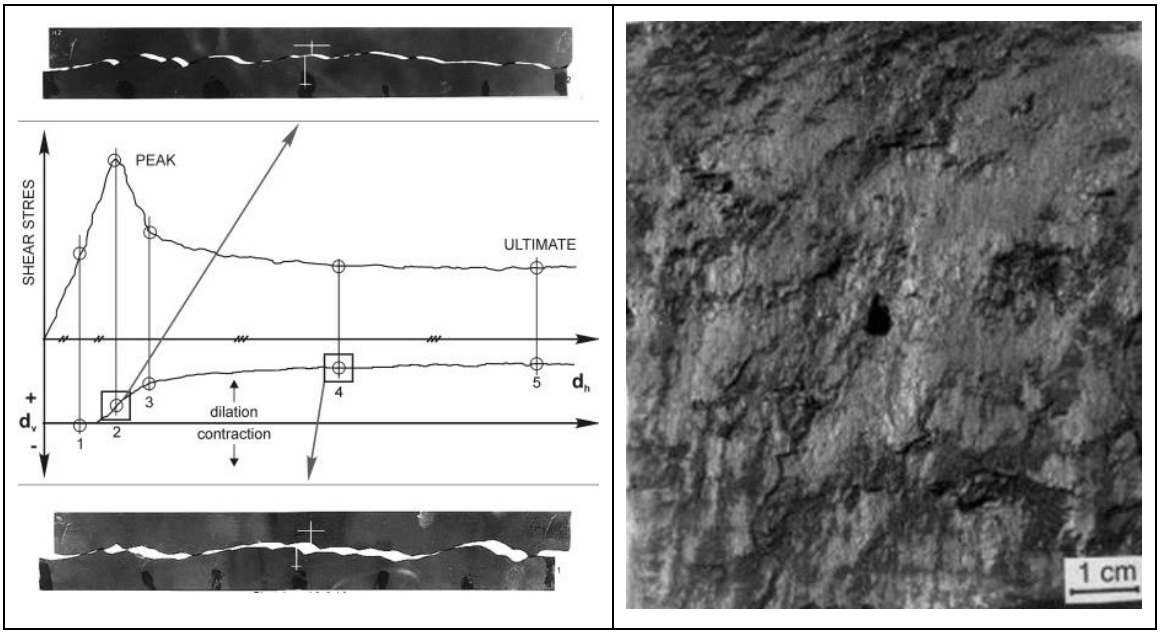

Figure 5 Left: Shear-dilation replication from direct shear tests on very rough tension fractures, from Barton, 1973, serve to illustrate but exaggerate the shear-dilation asperities-in-contact mechanisms. Right: The appearance of a sheared and flow tested natural fracture in Kimmeridge shale. The shale was weak and only 1 MPa effective normal stress was applied in this test. From Guttierez et al. 2000.

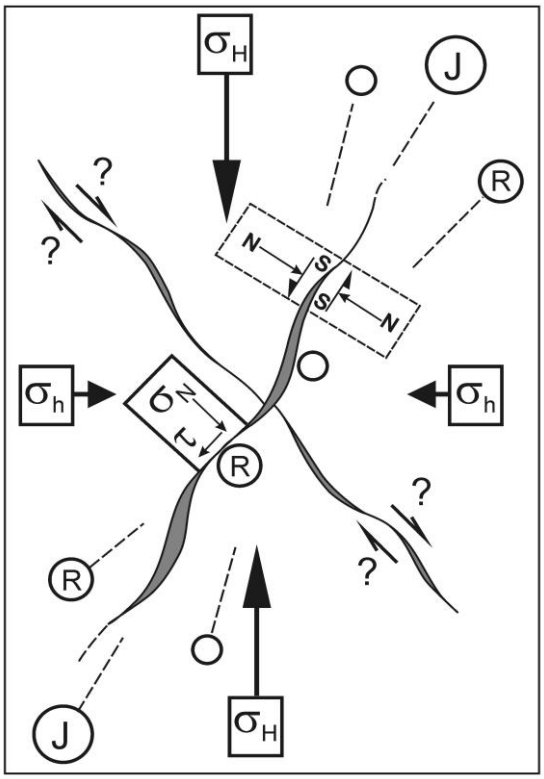

Figure 6 Members of two intersecting fracture sets shown with exaggerated roughness, and domination of shearing in one direction. Conceptually speaking, the contacting (R = rock-to-rock) highly-stressed portions of the fractures shown in the figure, will test the ability of a given shale to continue to produce as gas pressure reduces. Not only modulus as per Figure 1, but also JCS (wall strength) and non-linear matrix behaviour (Figure 2) will be important. From Barton, 2006, 2007a.

region, in order to gain surface area, appears to be the key to maintenance of flow, as stated in King, 2010. Detecting the location of natural fractures and optimizing their response to the 'central' hydraulic fracture stimulation volume, seems to be of prime importance. In practice, the shear stimulation (if it occurs), will tend to be dominated by the anisotropic nature of the bedding and jointing (Barton and Quadros, 2015), with shear on one set dominating as illustrated (in the context of non-stress-aligned shear-wave splitting) in Figure 6.

In the numerous early coupled shear-flow experiments performed on rock joints in the mid-eighties, approximately one to three orders of magnitude increase in conductivity was registered with only a very few millimeters of shearing (Makurat et al., 1990). Such increases also led to an understanding of the coupling of shearing and the almost maintained permeability (Barton et al. 1986, 1988), during the ongoing compaction of the Ekofisk chalk reservoir, which now exceeds 10 meters.

The CSFT (coupled shear flow test) developed by Makurat at NGI in the mid-eighties, also relied on the combination of sufficient static modulus E_{mass} and sufficient joint wall compressive strength JCS_n to maintain the effect of the shear-induced dilation. For dilation to occur at least some level of joint or fracture roughness JRC_n is required, despite the typical near-planarity often seen in shales.

Interesting and extensive joint-industry studies were more recently reported by respectively Texas A&M University and TerraTek/Schlumberger (Ghassemi and Suarez-Rivera, 2012). A selected and very small part of the reported (mostly hydraulic fracturing) studies reproduced in Figure 7 were concerned with the pressure-sensitive conductivity measured during the high-pressure flow tests through artificial saw-cuts or tension fractures in various shales. The latter were displaced 1 mm to (crudely) represent a 'sheared' fracture, based on the assumption that asperities would be crushed. Of course this does not produce the same result as CSFT (coupled shear-flow tests) as reported by Makurat et al., 1990. These more realistic tests were used in Ekofisk reservoir compaction studies, using natural fractures in the chalk. (Barton et al., 1988).

None of the surfaces tested at TerraTek/Sclumberger appear to have directly represented *natural fractures* in the shales, though judging (only) by the appearance of the three examples assembled in Figure 7, perhaps the saw-cuts were quite representative of the typical planarity of fractures in shale, assuming there were no traces of saw-cut 'ridges'. These authors assumed that conductivities poorer than approx. 0.01 md-ft would be too small to support flow at pressures > 2000 psi (≈ 14 MPa).

Ghassemi and Suarez-Rivera, 2012 actually concluded that unpropped 'secondary and tertiary fractures' (both of which were artificial in their studies) should be excluded from models. It is however not clear whether the TerraTek/Sclumberger/Texas A & M study tried also to quantify the potential contribution of aseismically-sheared fractures outside the hydro-fracked and propped region. This more difficult study with shearing of natural fractures, should ideally have also been the focus of attention, as it was in reservoir-compaction related studies using CSFT tests in the mid-eighties.

Rock mechanics appears to be very different from the *geomechanics* and *geoscience* practised by oil companies, their consultants, and by service companies. There is naturally much more focus on the deformability and strength of rock joints or rock fractures in rock mechanics, because these often determine the stability or otherwise, of potentially unstable opencast mine slopes, road cuttings, dam abutments, rock-wedges in rock caverns, etc.

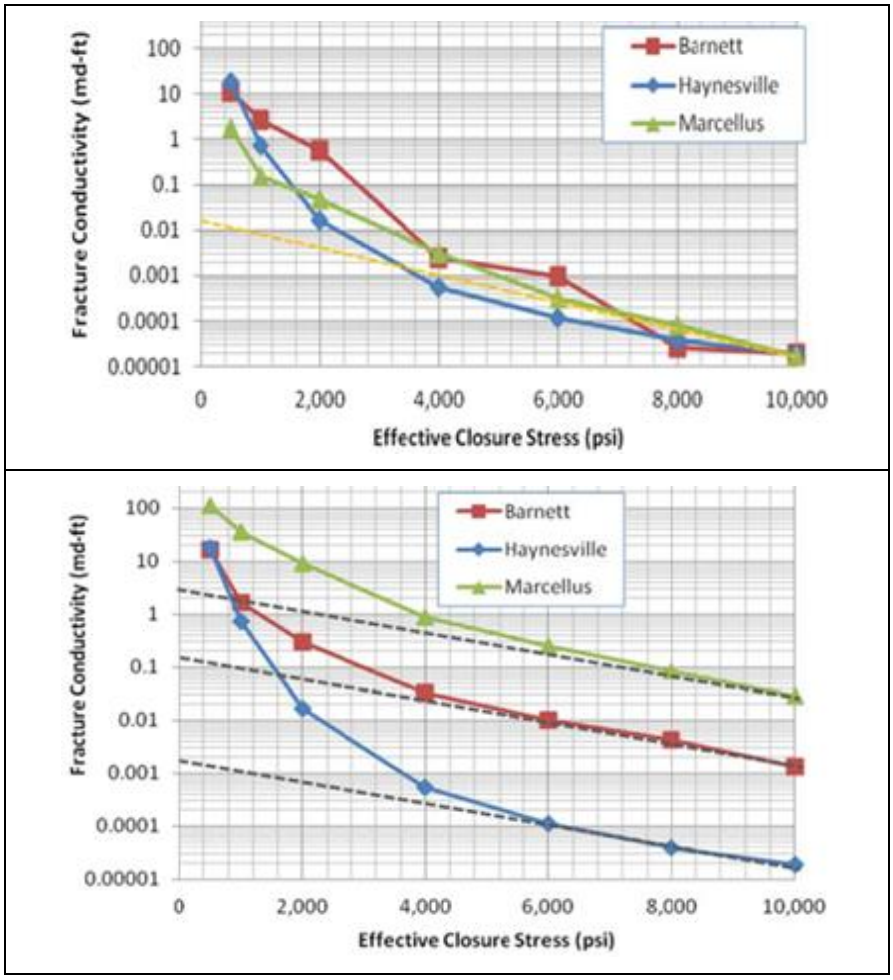

Figure 7 High pressure 'fracture' conductivity tests conducted (top): in saw-cut samples and (bottom): in 1 mm displaced-before-loading artificial tension fractures. Ghassemi and Suarez-Revera, 2012. The dotted lines show two decades of conductivity reduction over the increment of 69 MPa (10,000 psi) closure stress. Temperature increase reduced conductivity, presumably due to rock strength reduction. (In the case of natural fractures that are inter-locked, temperature improves 'fit').

The ability to model these discontinuous processes, also with coupling to conductivity and pore pressure, has been provided by distinct element (jointed) models such as Cundall's 2D UDEC (universal distinct element code) and by his 3D 3DEC, each marketed by Itasca. These codes have been in use for several decades. It would seem that they should have an important role to play in modelling the conceptual processes occurring in fractured reservoirs and gas-shales. (An example is Nagel et al. 2013). Both NFR and gas-shales rely on fracture deformation and coupling with permeability changes, so far little described in (linear) geomechanics.

4 Characterization methods for fractures in shale?

An essential step in this deformation-strength-permeability coupled (and non-linear) modelling process is the collection of input data for the constitutive joint or fracture behaviour modelling. The most widely used *non-linear* method, is the Barton-Bandis criterion described in Barton, 1982 and Barton and Bandis, 1990. It has been a part of UDEC-BB since 1985, and has been incorporated in 'competing' computer codes more recently. The necessary, but rapidly and cheaply obtained input data, is illustrated in Figure 8, with photographic examples in Figure 9.

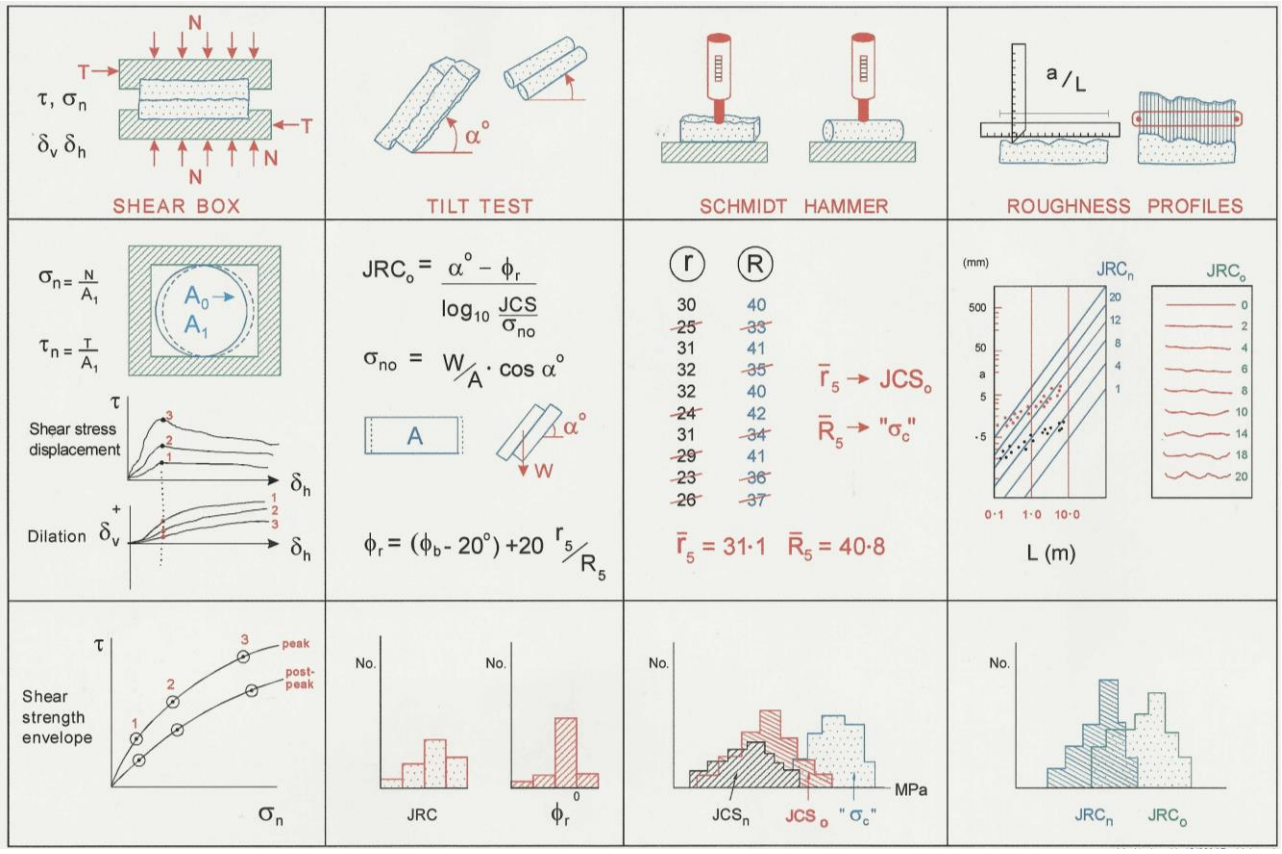

Figure 8 It appears that direct shear testing, as illustrated in the left column of this figure is extremely rare in oil companies and service companies. It is therefore not surprising that the roughness JRC and wall strength JCS parameters obtained by application of the illustrated drawings, are largely unfamiliar in oil company geomechanics teams. Barton, 1999 based on Barton and Choubey, 1977.

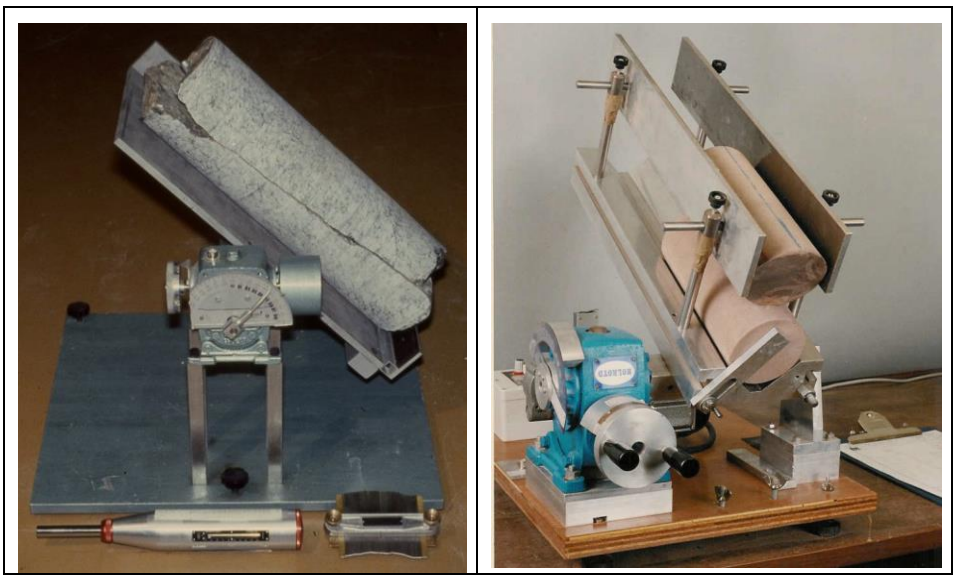

Figure 9 Tilt tests of natural joints for estimating JRC (as also performed on 3 km deep Ekofisk fractures in the mid-eighties), and tilt tests for estimating the basic friction angle of flat non-dilatant surfaces, using core 'sticks' in free-to-slide line contact. Also shown in the left-hand photograph are a Schmidt hammer for estimating JCS the joint or fracture wall strength, and a brush profilometer.

Extensive application was made of these parameters in the understanding of the Ekofisk fractured chalk compaction, in the mid-eighties. The oil company concerned had never before had people interested in studying the fractures. Nevertheless, the shearing-during-compaction revealed by our UDEC-BB modelling, not believed by many at the time, was later confirmed by the recovery of slickensided joints in the chalk, when planning large-scale seawater injection. Slickensides had not previously been seen during exploration 15 years earlier. These rock mechanics studies, which were performed by NGI with numerical assistance from Itasca, are described in Barton et al. 1986, 1988.

In order to give a feel for the magnitudes of JRC, which has proved to be block-size dependent (Barton and Choubey, 1977, Bandis et al., 1981), Figure 10 shows both small-scale and large-scale JRC_0 and JRC_n with the subscripts referring to nominal 10 cm and approx. 100 cm long samples. When core from the reservoir is (occasionally) available, tilt tests and back-calculation of JRC as shown in Figure 8 is recommended. If for example only drone-photographs of reservoir-analogue rock pavements or cliffs are available, then the measurement of roughness profiles, and a/L application (top-right, Figure 8) can be the alternatives. This amplitude/length (a/L) method involves placing a 1 m steel ruler, or shorter lengths of steel ruler, between surface asperity high points and measuring the corresponding amplitude (or 'depths' of the valleys). A 'cloud' of a/L measurements at different scale (L) can be used to convert to the relevant JRC_n value for

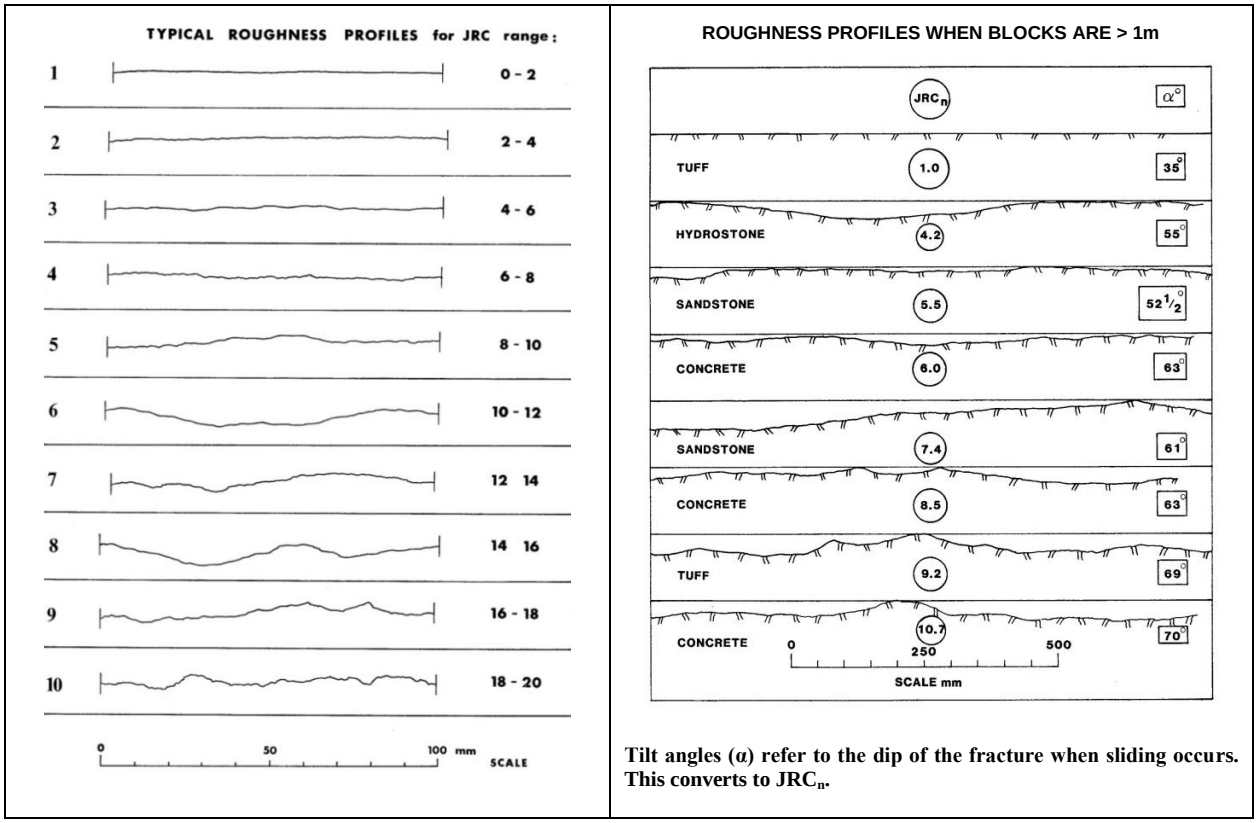

Figure 10 JRC at two different scales. These profiles can be used for matching to measured roughness profiles. However the recommended methods are tilt tests on core or on fractures recovered in sawn blocks from cliff faces, or a/L measurement as shown in Figure 11. The measured profiles (usually three per sample) and the shear-strength tested samples, are from Barton and Choubey, 1977 and Bakhtar and Barton, 1984. Of course today one has 3D laser profilometry from which to see roughness. Nevertheless a 'number' is still needed for numerical modelling.

block-size L_n. The relevant block-size for a given set of fractures is the mean spacing of the cross-joints or crossing fractures. The principle of the method is illustrated in Figure 11, demonstrating the scale effect as L increases.

5 Joint or fracture shear strength and deformability components

The tilt tests illustrated in Figures 8 and 9 are used to back-calculate the roughness coefficients JRC illustrated in Figure 10, using the Barton (1973, unweathered) or Barton and Choubey (1977 weathered) non-linear peak shear strength criteria. These were developed decades ago, in order to provide more accurate values of shear strength than the standard linear Mohr-Coulomb approximation. When in situ size blocks are involved, the block-size scaled *Barton and Bandis* shear strength criterion (Bandis et al. 1981) is used, with the subscripted parameters JRC_n and JCS_n signifying in situ (reservoir-estimated, pavement-estimated, or cliff-estimated) block sizes of nominal

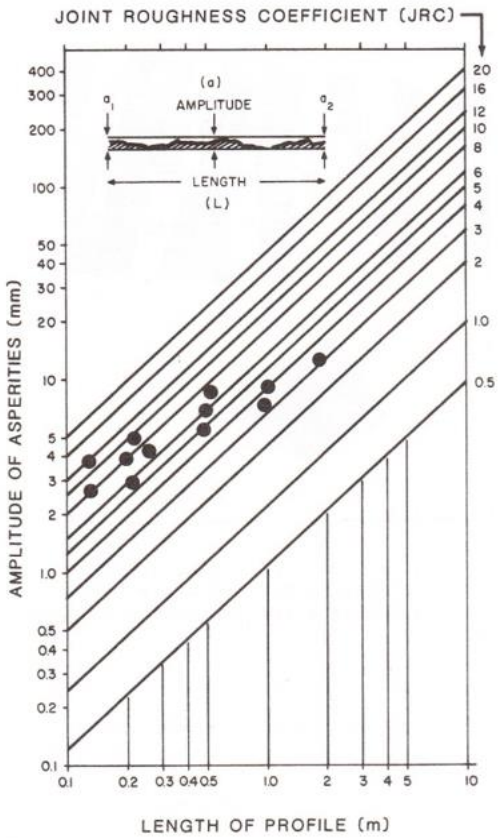

Figure 11 The a/L method for estimating JRC_n at different block size. This test is also very simple.

side-length L_n as compared to the nominal laboratory (core-sample) sizes of L_0. The three gradually improved non-linear, peak shear strength equations are listed below. They are direct decendents of two hundred direct shear tests on rough tension fractures developed in brittle model materials (e.g. Figure 5, left), in which 'roughness' was maximized at about 20, wall-strength was UCS (or σ_c since no weathering) and the basic friction angle was 30° (also because of no weathering).

$$\tau = \sigma_n' \tan [JRC \log_{10}(JCS/\sigma_n') + \varphi_b] \text{ (Barton, 1973)} \quad (1)$$

$$\tau = \sigma_n' \tan [JRC \log_{10}(JCS/\sigma_n') + \varphi_r] \text{ (Barton and Choubey, 1977)} \quad (2)$$

$$\tau = \sigma_n' \tan [JRC_n \log_{10}(JCS_n/\sigma_n') + \varphi_r] \text{ (Bandis et al.,1981)} \quad (3)$$

Note that the 'complicated non-linear term' $JRC \log_{10}(JCS/\sigma_{n'})$ provides the effect of both the stress-dependent *peak dilation angle* and the *asperity failure* component S_A which can be of almost equal (angular) magnitude. When generating shear-displacement-dilation-permeability coupling behaviour, the concept '$JRC_{mobilized}$' from Barton (1982)

is used. Some simple hand-calculated examples are given later in this paper. These methods may be the key to a quantitative understanding of gas-shale stimulation results. Of course they are also fundamental for production from 'critically stressed' NFR. We can move far beyond the Byerlee friction coefficients $\mu = 0.6, 0.85, 1.0$ favoured for so many years at Stanford University and by many oil and service companies, by using simple non-linear rock mechanics.

The above fracture roughness and strength parameters JRC, JCS and φ_r allow one to generate the desirable *shear-dilation-permeability* enhancement curves, as probably operating in stimulated gas-shales, and the much less desirable *stress-closure-permeability* non-enhancement curves, which make themselves known in stress-sensitive reservoirs, or later on in the life of a producing reservoir. This type of non-linear, rock mechanics based 4D coupled behaviour modelling seems to be rare or absent in petroleum geomechanics. Great sophistication is seen in many other areas but apparently not in this area.. (If it is in fact occurring but is not published due to confidentiality rules, then the present article could perhaps be considered a contribution to the 'open literature').

Experimentally measured examples of joint or fracture-closure and shear are illustrated in the top of Figure 12. The top two diagrams illustrate measurements (from Bandis et al., 1981, 1983), of normal stress-closure, and shear-displacement tendencies for jointed blocks of different sizes. Note the scale effect, which is most prominent when joints or fractures are rough. Chryssanthakis et al. 1991 reported the UDEC-BB modelling shown at the bottom of Figure 11.

In the central diagram, use of these deformation components were applied by Barton,1986, in order to predict the relative strengths of the normal-closure component, which was now termed N, and the shear component which was now termed S. We must anticipate that something 'similar' is happening when gas-shales are stimulated. We would like the Type A (sedimentary) rock mass to display as little as possible of the N-component (closure) following helpful excursions into microseismically signaled S-component behavior.

As mentioned earlier, whether we can 'delay' the N-component and increase production time, will depend on three things: sufficient JCS, sufficient static deformation modulus ($M \approx 10\ Q_c^{1/3}$ if using V_P related Q-values: Barton, 2006, 2007b), and how far around the matrix shear-strength envelope one has progressed (Figure 2), particularly at the most stressed fracture asperity rock-to-rock contacts.

Figure 13, from Barton, 1982 demonstrates another important property of rock masses, which has potential application to understanding the process of gas-shale stimulation: namely the quite low shear stiffness which is also related with *in situ* block size. To be strictly correct this should be termed the *peak shear stiffness*, which is shown defined in Figure 12, left-inset.

6 There is more to fracture shearing than a single friction coefficient

This direct challenge to the conventional geomechanics application of a 'single-value' of the friction coefficient (μ) popularised in the USA by Byerlee, 1978, C.Barton et al. 1995, Zoback and Townend, 2001, and even Zoback, 2007: a comprehensive book on reservoir geomechanics, is deliberate. It is believed that the non-application of non-linear rock mechanics, as evidenced by geomechanics teams in oil and service companies, is considered to be a negative continuing influence. At first of course, the recognition, also in the US, that shearing could be associated with permeability/productivity, was a positive step.

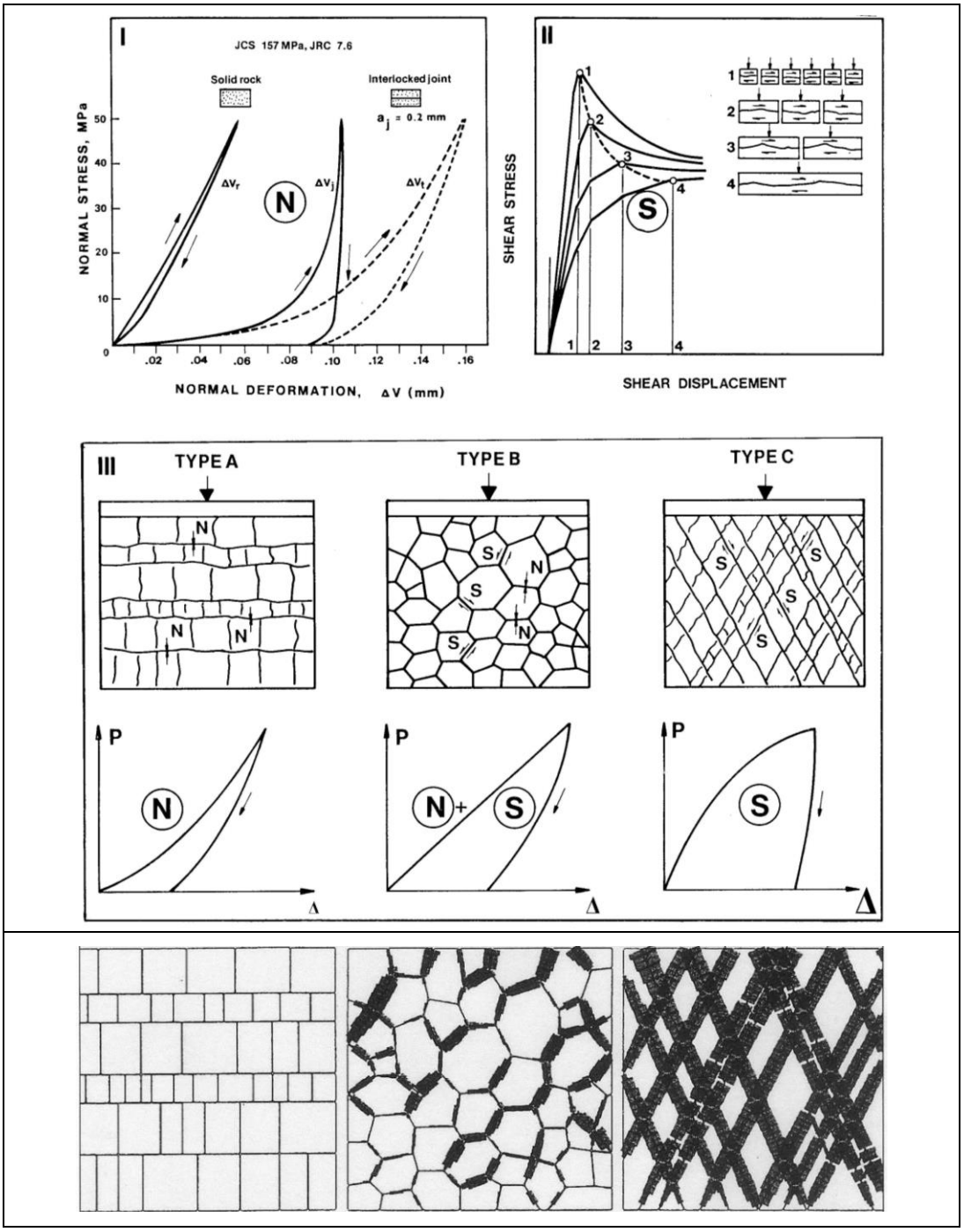

Figure 12 Some basic deformation modes of rock masses caused by specific combinations of the non-linear (concave and convex) joint deformation components N and S. The UDEC-BB models (bottom) show the relative strengths of the (black) shear component, whose strengths would also signify flow potential. So S would be favourable and N unfavourable, for drainage towards the 'central' propped region in the context of shale-gas production, assuming fracture deformation is needed to assist in this drainage of an almost impermeable (when undisturbed) medium. Based on Barton, 1986.

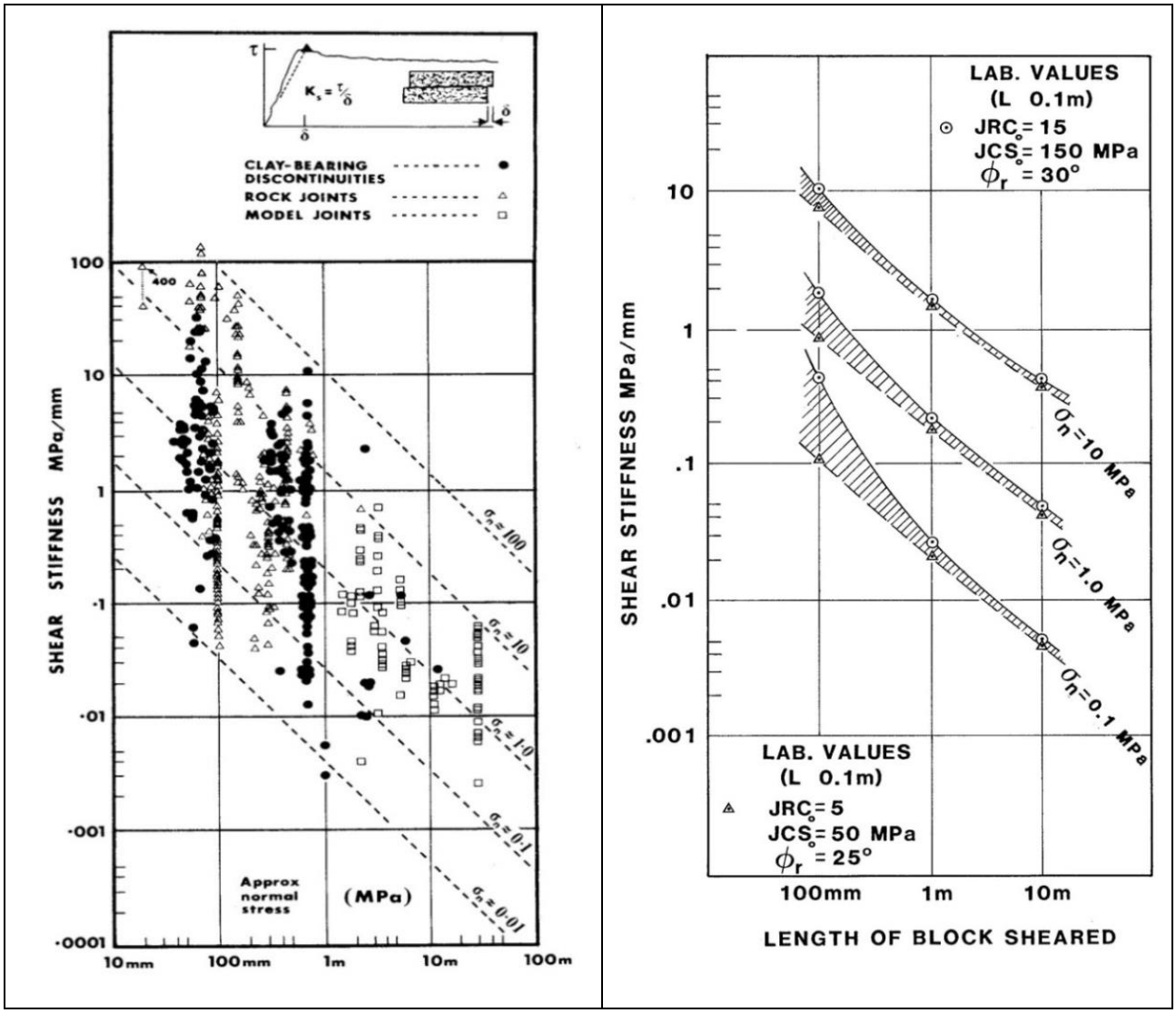

Figure 13 The inset (left) shows how shear stiffness (Ks) is estimated. This important parameter is strongly affected by all three 'joint parameters' (JRC, JCS and φ_r), and is doubly (block-size) scale-dependent, due to peak strength and displacement-to-peak scale dependency, as described in Barton (1982) and Barton et al. (1985). The parameter Ks is probably fundamental to oil shale and gas-shale stimulation success or failure.

An essential part of coupled process modelling involving joint or fracture shearing, is the ability to track shear deformation and dilation up to and beyond peak strength, and the associated physical aperture changes. The latter can be converted to permeability. This of course is more useful than estimating a single peak value of strength. The JRC (mobilized) dimensionless model shown in Figure 14 was first published in Barton, 1982, while working at TerraTek (now Schlumberger) in Salt Lake City. The version illustrated is from Barton, 2006 (Chapter 16 concerning shearing processes in rock mechanics). When one conducts direct shear tests on different joint or fracture samples at widely different normal stress levels, a series of widely differing shear stress-displacement (and dilation-displacement) curves are obtained. The dimensionless quantities (JRC_{mob} / JRC_{peak} and δ/δ_{peak}) represented in the 'unifying' diagram shown in Figure 14, has the effect of consolidating experimental shear stress-displacement test results into one narrow band, with

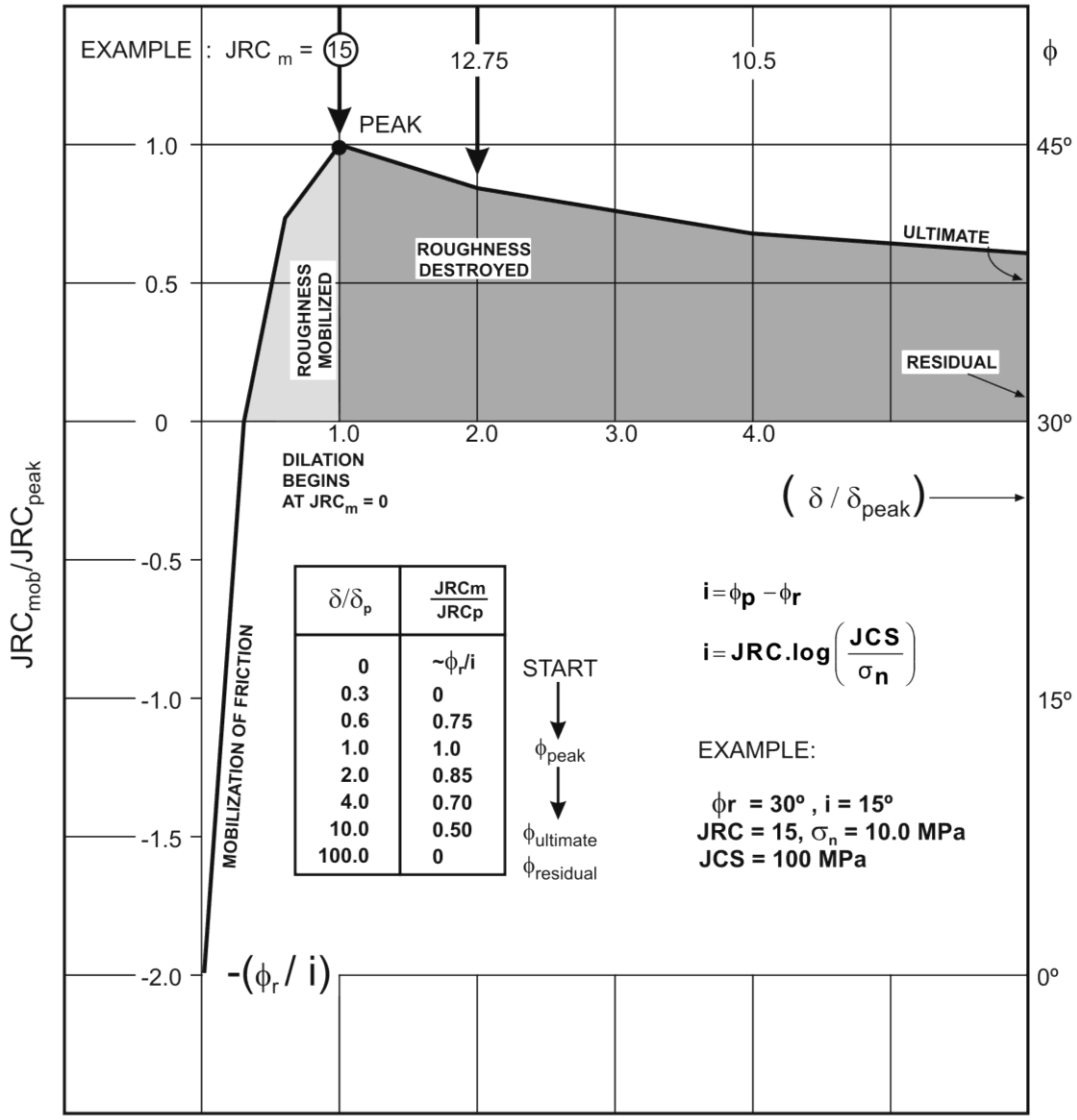

Figure 14 Peak shear strength for fractures, as epitomised by a friction coefficient (0.85 according to 'Byerlee's law' for stress levels above 5 MPa, but less than 25 MPa) is not so simple as this, which is fortunate for shale-gas drainage. This figure shows the dimensionless JRC (mobilized) concept of Barton, 1982 on which part of the Barton-Bandis criterion was based. Peak strength has to be reached by some deformation and dilation, meaning also permeability increase. Post-peak, JRC (mob) reduces.

the approximate shape shown in the figure. (The 'look-up' table of values: see inset, is of course smoothed by using more coordinates, in the computerized UDEC-BB sub-routine, dating from 1985.) We can therefore use this simple device to generate widely different shear stress-displacement and dilation-displacement curves for any desired input data (including variable block size and variable effective normal stress, as shown in Figure 16.

An important and favourable feature of stimulated production of gas-shale is that the shear strength of rock joints or fractures is block-size dependent, as shown in the hand-calculated demonstration (Figure 15) also from Barton, 1982. Shearing may be 'easier' than expected. Note that the space created for flow by shearing-induced dilation will be compromised at high effective normal stress, due to reduced dilation and possible/probable gouge production.

It will be noticed that a dilation ‘delay’ is involved. (When block size is larger this is easier to see). This may be something to consider when stimulating gas-shales. In other words a significant fracking and propping is needed in the ‘central’ ellipsoidal volume to push the surrounding shale beyond the ‘dilation delay’. However, only a very few millimeters of shear is needed to greatly enhance the potential permeability. The models shown in Figure 16 are without any gouge correction, but the physical/hydraulic aperture (E/e) conversion (described later) already corrects for the tortuosity/out-of-plane flow effects of rock-to-rock contact across the stressed joints or fractures.

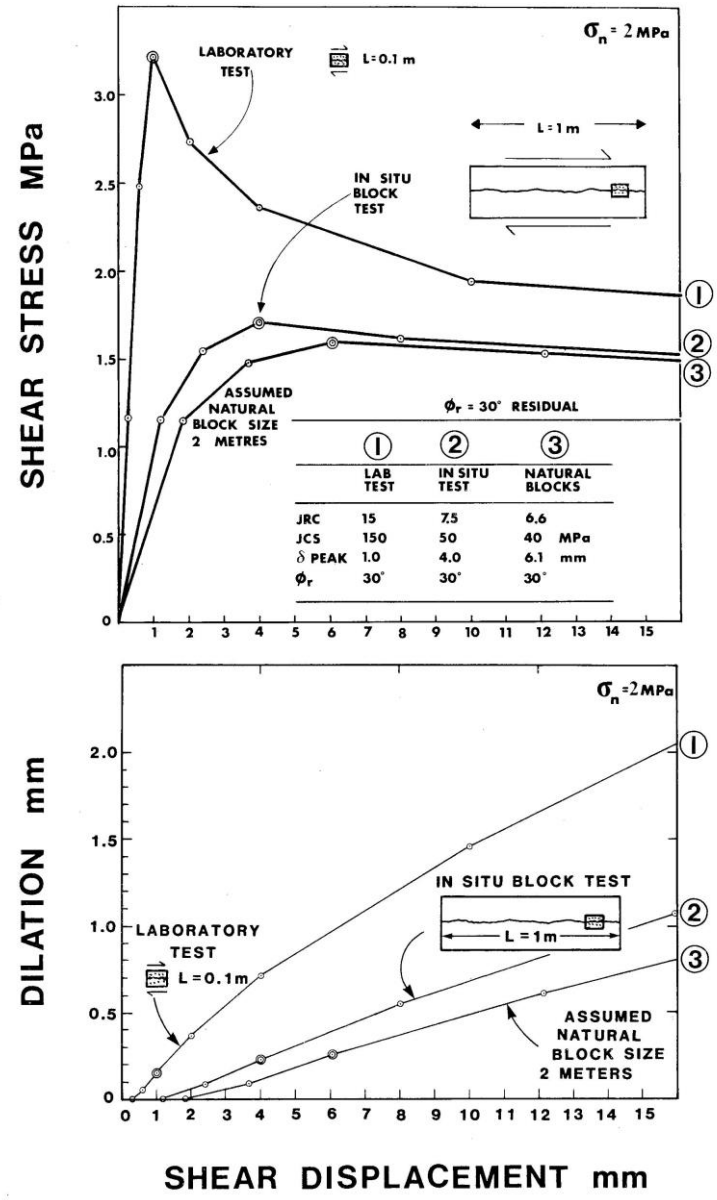

Figure 15 Stress-displacement-dilation behavioural trends, generated using the JRC (mobilized) model. This has been done for three different block sizes (0.1, 1.0 and 2.0 m) to demonstrate the strong scale effect seen when fracture roughness is significant. Barton, 1982 and Barton et al. 1985.

The series of BB coupled-behaviour models shown in Figure 16 could be generated on an HP programmable calculator by Bakhtar in 1983, while he and the writer were working in TerraTek (now Schlumberger) in Salt Lake City. This was part of a two-volume nuclear waste related study for AECL/CANMET in Canada.

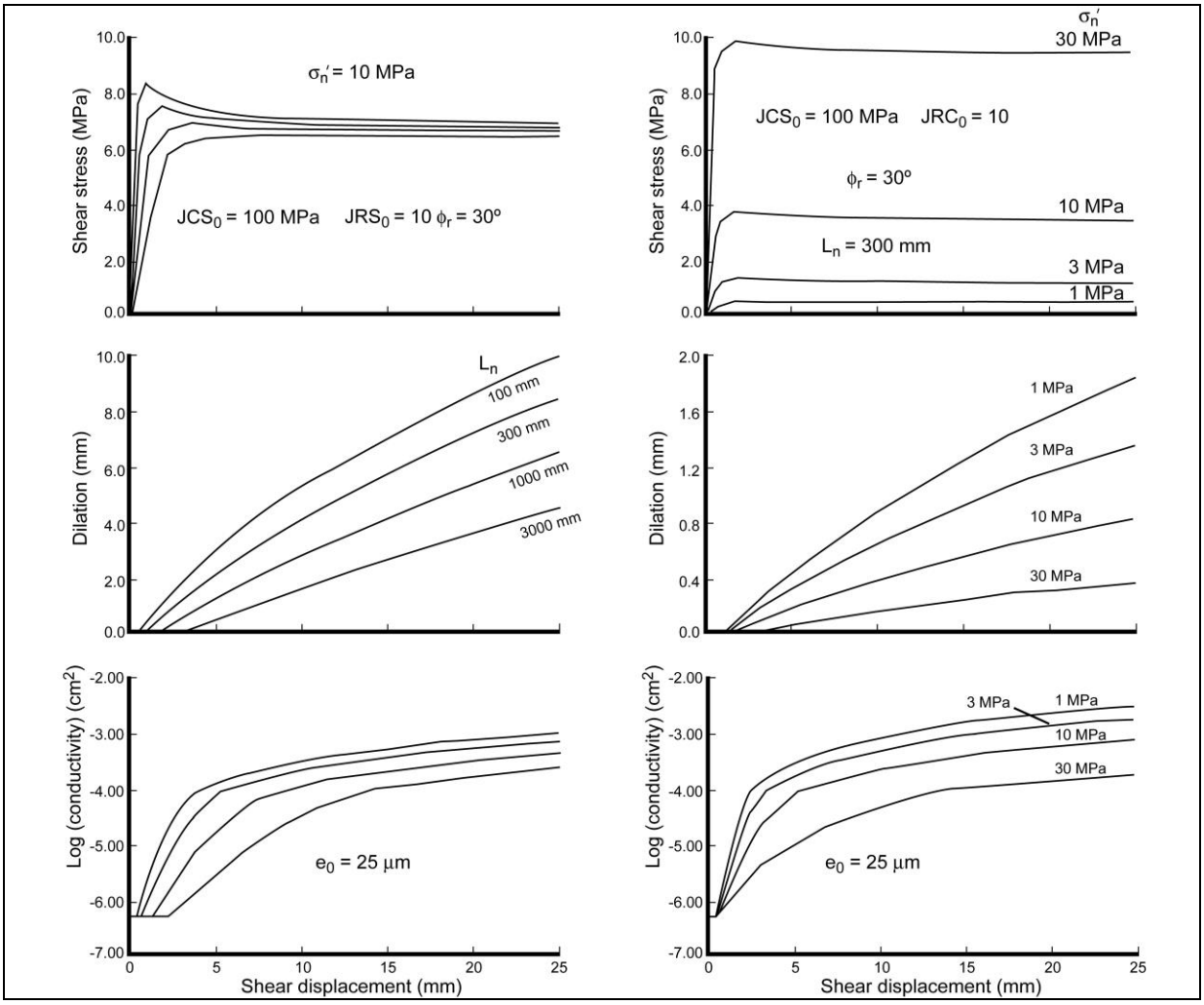

Figure 16 Demonstration of Barton-Bandis shear strength-dilation-permeability coupling, with scale effects (left) and effects of varied normal stress (right) taken into account. Barton and Bakhtar, 1983.

The sets of three curves on the left and right are designed to demonstrate the likely effect of block size (0.1, 0.3, 1.0 and 3.0 m), and the effect of effective normal stress (1, 3,10 and 30 MPa at constant block-size of 300 mm). The latter is possibly of shale-like block size. Note that the third or lowest set of curves in each case are based on the empirical conversion from physical aperture E to hydraulic aperture e, with an assumed starting point, for these examples, of e_0 = 25 μm. In practice, due to the $JRC_{mobilized}$ mechanism and possible gouge production, the increased conductivity with shear deformation may be less than graphed here, but is likely to remain impressive at least while the shale remains brittle or nearly brittle.

7 Coupling of fracture deformation with permeability

The coupling of the desirable *shear-dilation-permeability* and the undesirable *normal closure-permeability*, and the differentiation of hydraulic (e) and physical (E) joint or fracture apertures, is occurring 'in deep back-ground' in UDEC-BB numerical modelling. It has been part of rock mechanics modelling since 1985, and it would seem to be applicable in the petroleum industry, if not already used, especially with the recognition of so much 'remaining' production (perhaps > 60%) from fractured and unconventional (shale) reservoirs. It was used first in the mid-eighties in our investigations of the Ekofisk reservoir compaction in offshore Norway.

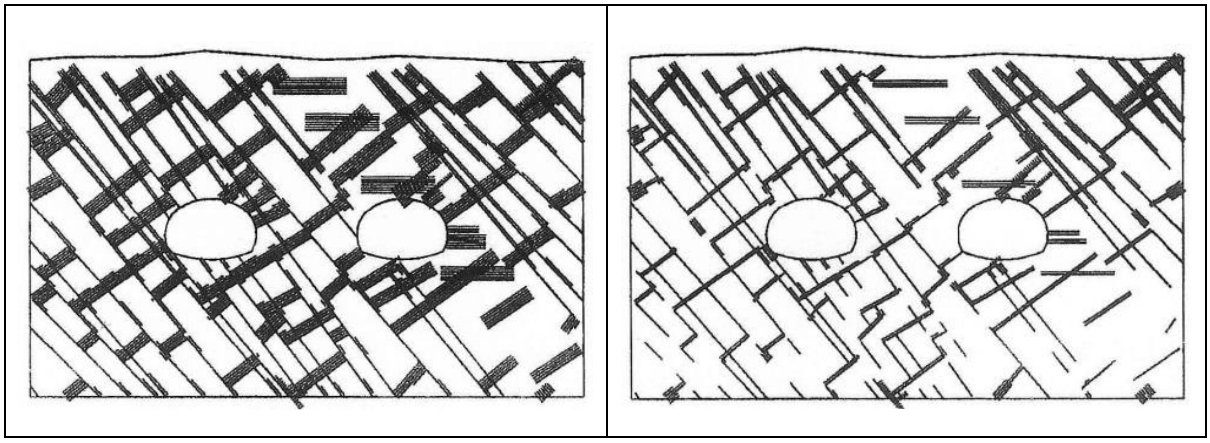

Figure 17 UDEC-BB model of twin tunnels in limestones and shales, from Makurat and Barton (1988). Note the stress or depth dependence, due to closure of apertures (N component of Figure 9).

Figure 17 is an example of coupled UDEC-BB modelling from a different field than reservoirs. Nevertheless it is a convenient way to demonstrate the depth or stress dependence of the two apertures E (physical: left diagram) and e (theoretical smooth-wall hydraulic: right diagram). Note that shearing-induced dilation or tensile opening can open the physical aperture sufficiently for e and E to be equal. This usually occurs when apertures reach approximately 0.5 to 1.0 mm, as can be seen in Figure 18, for the case of the larger (rougher-walled) JRC_0 values. Both apertures will probably be extremely small (a few microns size) at kilometers depth in gas-shales, until shearing and (slight but sufficient) dilation occurs. Fracture aperture E (physical) is tracked in the non-linear Barton-Bandis model, and converted to e (hydraulic aperture) based on the JRC_0 dependent conversion from E to e shown in Figure 18. Permeability, or more correctly joint- or fracture-conductivity is determined by the smaller hydraulic aperture (e) (with $k = e^2/12$), unless the matrix is significantly permeable as well.

In the present context of reservoirs, petroleum reserves lie in the matrix pores and in the larger physical joint- or fracture-apertures (E), especially in the case of fractured basement reservoirs in granites, which have high fracture porosity and low matrix porosity. The apertures which can be back-calculated from flow tests or from interpretation of production are the usually much smaller hydraulic apertures (e), so reserves in basement fractured reservoirs need to be greatly upgraded if the E > e mismatch has not been allowed for (Barton, 2014b).

Conversion between physical and hydraulic apertures was a subject that pre-occupied the author a long time ago. In Barton, 1972 a graph was shown in which recent tests conducted at the University in Trondheim were interpreted such that the ratio of E/e could be expressed as a function of the hydraulic aperture (e). Later in Barton, 1982 more data was collected and interpreted showing that the small-scale roughness JRC (strictly JRC_0) had an important role to play in the ratio E/e. This is logical as JRC can be estimated from the ratio of roughness amplitude (a) and length of profile (L), therefore being equivalent to relative roughness in hydraulics, though at much larger scale. The data of e, E and JRC was further updated in Barton et al. 1985, and later by Quadros, as reported in Barton and Quadros, 1997.

Figure 18 (top) shows the empirical model for converting between e and E in the case of normal closure. In the case of shearing with possible gouge production (Figure18, bottom), the E/e data inclines from left down to the right, crossing the coloured curves shown in the top diagram. *In situ* block test data involving some shearing had suggested this in 1982, but a formal improvement in the model converting E to e and vice versa, was not published until Olsson and Barton, 2001. This followed Ph.D. studies of Olsson, which were externally examined by the writer. The term $JRC_{mobilized}$ was suggested in the new conversion of e to E for the case of shear. So we have the two forms:

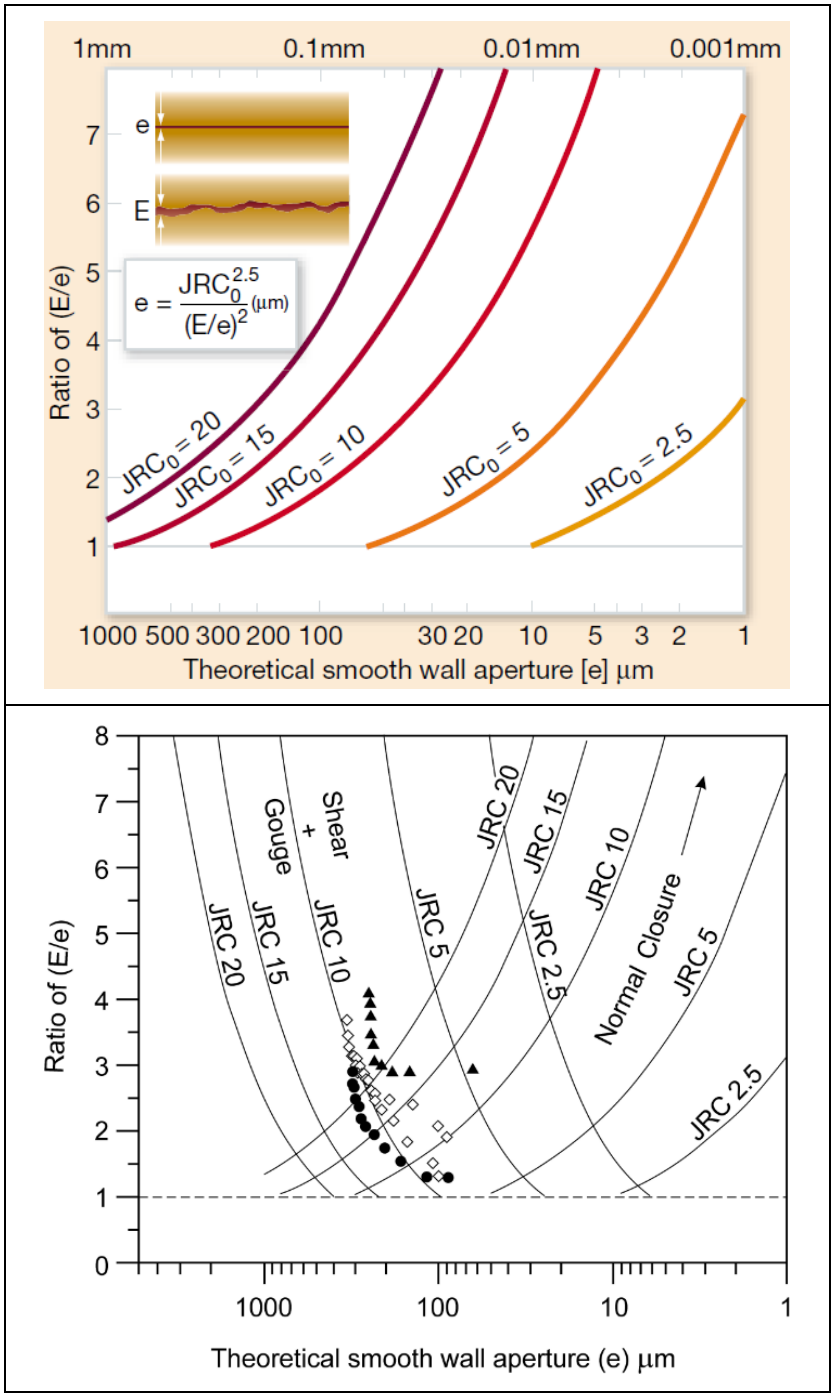

Figure 18 Top: This E/e conversion (from Barton, 1982) applies to normal closure. When shear (and possible gouge production) is involved: Bottom: a modified form of E/e conversion is used (Olsson and Barton, 2001), using the 1982 JRC $_{mobilized}$ concept. In practice, when shearing occurs, the 'JRC-curves' are steeper and incline upwards to the left instead of up to the right as in the original normal closure model. JRC $_{mobilized}$ tracks the mobilization of roughness pre-peak and the degradation of roughness post-peak.

1. For normal closure: $e = E^2/JRC_0^{2.5}$ (4)

2. For shear (and possible gouge) : $e = E^{1/2}\ JRC_{mob}$ (5)

In situ block test data described in Barton, 1982, and laboratory shear-flow data from Olsson (Olsson and Barton, 2001) gave evidence for the need for this adjustment for shear, with possible permeability losses due to gouge. Note that the permeability eventually increases most in the direction perpendicular to the shearing direction, as suggested and demonstrated by Gentier, 1987 in the late eighties.

Also using the physical aperture to conducting aperture conversion (but pre-dating the Olsson and Barton, 2001 conversion), Figure 19 illustrates one-dimensional compaction modelling of a representative, vertical-section, 1 x 1 m 'window' representing porous-and-jointed parts of the massive 14 x 9 x 0.3 km Ekofisk reservoir in the North Sea. Some conceptual modelling along these lines for the case of gas-shale may give useful insight, if realistic boundary conditions can be transferred from larger-scale 3D models of the hydraulic fracturing and proppant (no-closure) behaviour. No doubt there are research establishments which have been attempting this, but not publishing their findings. Some indications of some on-going distinct-element modelling work for gas-shale were given by Nagel et al. 2013. Much more is surely needed for conceptual understanding.

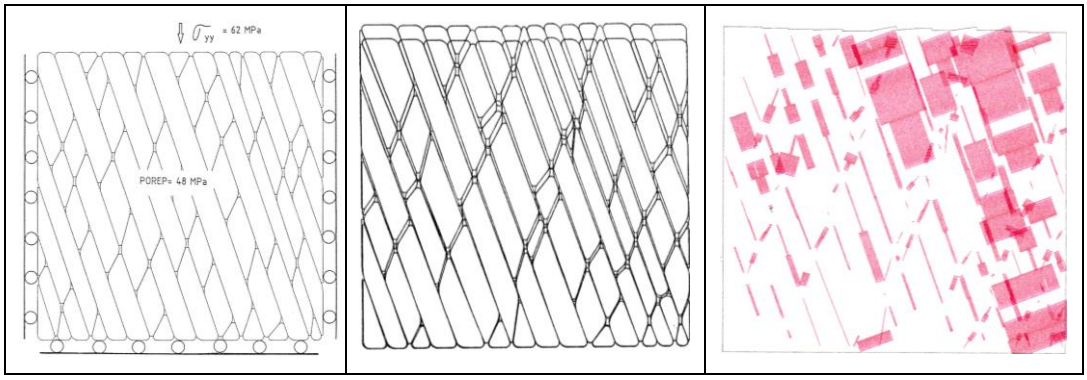

Figure 19 Discrete element (jointed) model of a '1 m window' in the porous and jointed Ekofisk chalk, loaded by reducing the pore pressure from 48 to 28 MPa. This caused some shrinkage of the matrix, which made space for joint shearing despite the ID roller-boundary compaction restraint. From NGI-Itasca modelling, reported in Barton et al. 1988. (Each red line represents 50 μm of shearing, with maximum of 3 mm in this model).

In this conceptual NFR model 'unit' (Figure 19), there is a maximum of 3 mm of fracture shearing. In further studies at NGI using 24 MPa reduction in pore pressure and a different geometry for the conjugate fractures, a maximum 10 mm of shear was modelled (pers. comm. M. Gutierrez). In the case of the gas-shale, the compaction of pore space will be much more limited, and mechanical (rock mass deformation caused by the massive fracking may be needed.

Jointed/fractured cores of Ekofisk chalk recovered by Phillips were sampled by the author from core stored in Bartlesville, during NGI's project for the Norwegian Petroleum Directorate. The joint/fracture samples were characterized as illustrated in Figure 8, in order to derive representative values of the three strength parameters JRC_n, JCS_n and φ_r. See Barton et al.1986 and 1988. Note that the modelled shearing, shown by 'flag-thickness' is anisotropic, and clearly not parallel to the vertical applied principal stress. Conceptually it resembles Figure 6 anisotropy.

As a matter of 'proof of shear', *slickensided* polished joints were reportedly recognized by Phillips geologists (pers. comm. Helen Farrel), in recovered core from the mid-eighties Ekofisk water-flooding project. Such features had not been seen during exploration 15 years before. As also with gas-shale, some shearing is the key to enough dilation and the development and maintenance of some measure of permeability and therefore gas drainage. The Ekofisk reservoir is expected to produce for 80 years, no doubt with the help of a lot of fracture shearing, not just 'rubbleization' and 'compaction drive' as presumed by some of those involved at the time.

8 Is slip area misinterpreted?

The 'clouds' of microseismic events recorded by Warpinski and colleagues, examples of which are given in Figures 20 and 21, represent very low-energy (low moment) events. The definitions of the moment and magnitude of an earthquake, which apply to microseismic events as well, are based on:

$$M_0 = \mu dA \qquad (6)$$

where μ is the shear modulus, d is the slip distance and A is the area of slip.

Perhaps due to a focus on showing the insignificance of the shear displacements, these authors 'composed' examples of slip area (or radius) that seem high, giving (through equation 6) displacements that seem very low. These low magnitudes (of slip energy dissipation) can imply a range of (large) fracture radii of e.g. 6m to 11m, slipping only 0.69 to 0.74 μ, with assumed shear modulus μ typically from 5 to 25 GPa. If on the other hand the interpreted slip is more closely related to fracture slip in shale with much smaller (but more numerous) *block-size related fracture sizes,*

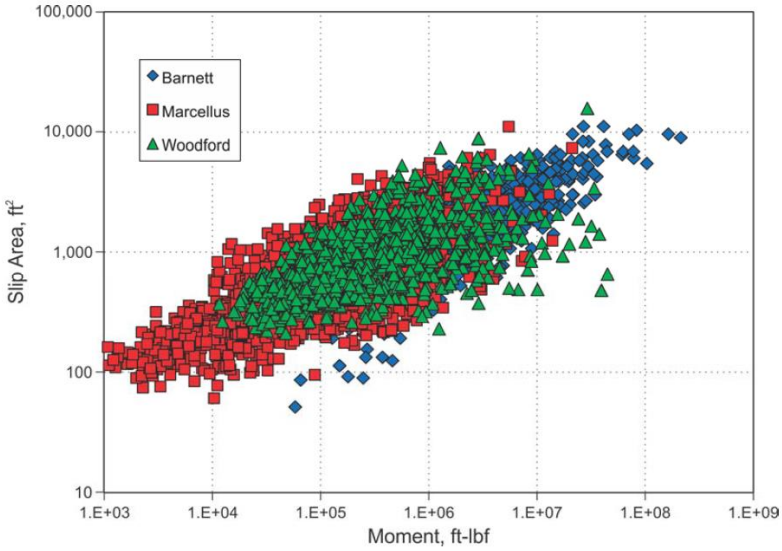

Figure 20 Examples of possible combinations of slip areas and moments. Warpinski et al., 2012. If d had been made much larger and more realistic, the slip areas would also have become more realistic.

then the estimated slip can easily be ten times larger, and amount to, for instance, 10-times the pre-shear micron-size *fracture apertures.* The assumed slip magnitudes seem more likely to be associated with breakage of weak cohesive 'mineral' bonding, requiring very small slip magnitudes, while the much larger slip magnitudes needed for permeability development could presumably be *aseismic slip*.

It seems probable, though is an unknown, that *aseismic* slip much larger than '5-10 micron-size', can continue to stimulate the gas drainage, due to the ease of shear when there is only slight dilation. As shown in Figure 13, *in situ* shear stiffness is potentially and helpfully, likely to be rather low. However, will the shale be strong enough to remain 'naturally shear-propped'? This depends on the pressure draw-down in relation to JCS and Figure 2 behaviour (non-linear), as applied to the critical rock-to-rock contacting highly stressed opposed fracture walls. Figure 5a, with exaggerated roughness, could be used to assist in visualization of the contacting asperities, but when roughness is limited, areas in contact will (fortunately) be far larger, so stress levels will be lower. It is apparently a behaviour which is in delicate balance. Enough dilation (i.e. non-planarity of the fractures) is needed to greatly enhance the extremely low initial permeability, but not enough to act as significant stress raisers.

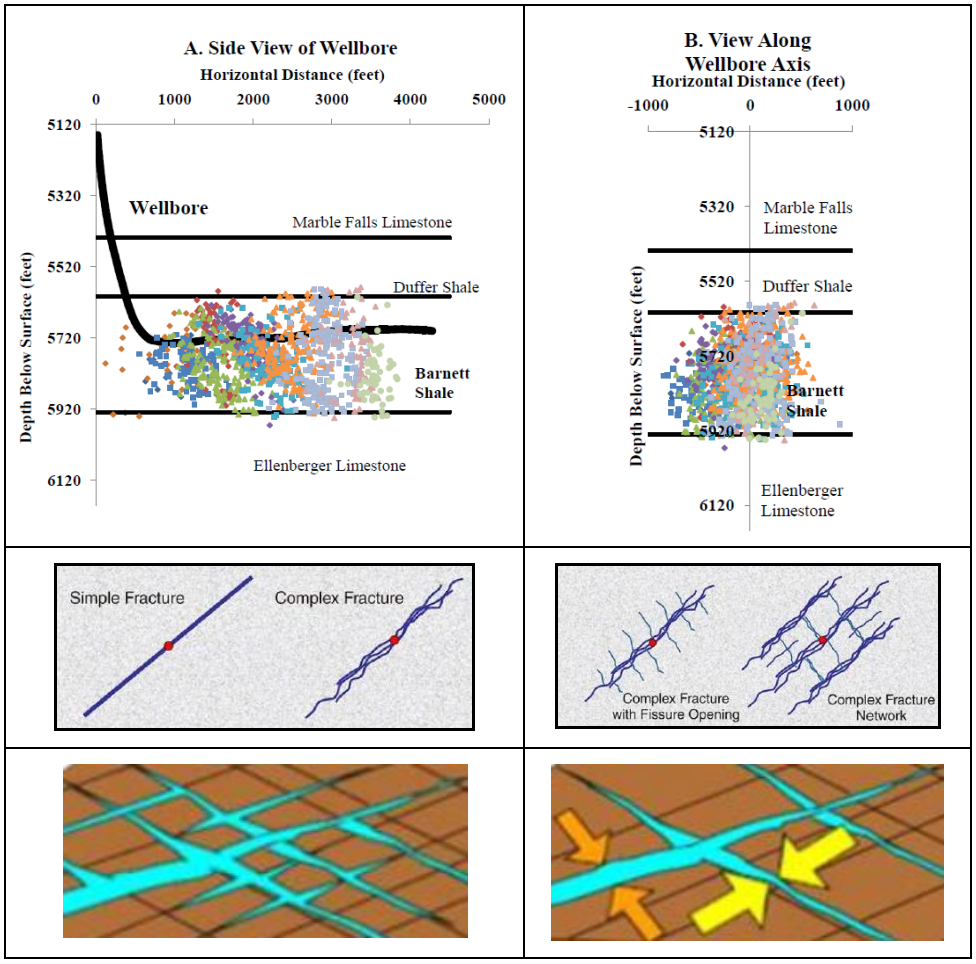

Figure 21 Top: Microseismic resulting from hydraulic fracturing in the brittle Barnett Shale, USA signifies shearing of fractures, each colour representing recordings due to a distinct fracturing stage. (Zoback et al., 2010). This micro-seismic data does not represent the hydraulic (tensile) fractures illustrated in the six sketches. Centre: Schematics of assumed levels of complexity of hydraulic fractures, as occasionally observed in mine-backs. (Fisher and Warpinski, 2011). Bottom: Modified from sketches in Mclennon and Potocki, 2013 concerning the influences of multi-fracked branches on ISIP (instantaneous shut-in pressure) due to the attempt by two of the principal in situ stress components, to force fluid back to the perforations, also closing tightly against the proppants.

9 Conclusions

1. Based on presentations made in several workshops and courses attended on both sides of the Atlantic in the last seven to eight years, the writer has gained the strong impression that *geomechanics*, complex enough as it is, seems to be mostly practiced in the petroleum industry without considering the application of *non-linear* rock mechanics.

2. Since microseismic activity significantly outside the hydraulic fracture-stimulated zones is apparently registered, and since this activity is shear-induced, the production of shale gas depends more strongly than usual on a coupled-process of shear strength-dilation-permeability-stress interaction, with non-linear rock mechanics input as an essential component.
3. It is not sufficient to invoke linear Mohr-Coulomb geomechanics when both the fractures and matrix are to go through many tens of MPa stress change during even one year of first-stage production. Non-linearity and the

problem of reaching the brittle-ductile transition and perhaps critical-state may arise in the lower modulus lower strength shales, and it will arise first in the stress-transferring 'island-asperities' which are sustaining shear displacement.

4. Non-linear shear strength, dilation and permeability coupling of joints and fractures, with in-built scale effects, is likely to give a more realistic prediction of gas-shale stimulation performance, than anything limited to Byerlee friction coefficients or linear Mohr-Coulomb. The over-frequent use of these simplified models needs review since we are talking of an industry dependent on future production from mostly (at least 60%) fractured reservoirs.
5. Inevitably there may be impressive ongoing rock mechanics modelling of the non-linear coupled processes, as briefly discussed in this paper. This may be occurring in some large oil and service companies, or in sponsored university departments. The fact that such work is not readily published or described in workshops means that the author must apologise to those who cannot easily respond to say 'we have also been doing that'. Nevertheless, it would be nice to know if it is happening.

Glossary of terms to aid in cross-discipline communication

PARAMETER	DEFINITION
c	The cohesive strength of intact rock (assuming linear Mohr-Coulomb strength envelopes). A non-linear alternative is proposed.
φ	The frictional strength of intact rock (assuming linear Mohr-Coulomb strength envelopes). A non-linear alternative is proposed.
JRC, JRC_n	Joint- or fracture-roughness coefficient (typical range 0 to 20 from completely smooth-planar to rough-undulating). Scale-dependent. The block-size scaled-value of JRC_n has lower values.
JCS JCS_n	Joint- or fracture wall strength (typical range 10 to 150 MPa from weak-porous to hard non-porous rock). Scale-dependent. Experience with gas-shales suggests the need for brittle behaviour (also meaning higher JCS) lasting as long as possible, while effective stresses are low enough to prevent the brittle-ductile transition being reached.
r, R	Schmidt-hammer rebound (mean of *top* 50% of tests) on respectively the saturated joint or fracture wall, and on the dry unweathered rock. The ratio r/R describes the degree of fracture-surface weathering/alteration.
L_0 and L_n	Nominal laboratory-sample length, and *in situ* block size or spacing of cross-joints (cross-fractures). In case of anisotropic fracture spacings, tabular block shapes may require two estimates of L_n.
φ_r	Residual friction angle of a joint or fracture after a significant amount of shearing. Ultimate strength is reached earlier, at the end of a shear test. (Typical range of minimum φ_r is 24° to 28° when clay-coatings are absent).
$JRC_{mobilised}$	The shear-displacement-dependent mobilization (and post-peak degradation) of the joint roughness coefficient. This demonstrates that frictional strength is not so elementary as single (peak values) of $\mu = 0.6$, 0.85 etc. pioneered long ago by Byerlee and widely used in the USA.

δ and δ_{peak}	The ongoing shear displacement, and the shear displacement needed to reach *peak* shear strength, which reduces to < 1% of *in situ* block length when block-size exceeds approximately 100 mm.
σ', σ_1, σ_3, and σ_n'	Effective stress, axial (major) stress, confining (minor) stress, and normal effective stress across a joint or fracture.
K_n and K_s	Normal and shear stiffness of joints or fractures. Both are stress-dependent and non-linear. K_s is also block-size dependent (it is therefore lower in situ). The ratio Kn/Ks may be from 10 to 100.
Q-value, Jr, Ja	These terms have been used in the world of tunneling for the last 40 years, describe rock mass quality, joint roughness and joint alteration or clay-filling. Q correlates to the stress-dependent static deformation modulus E_{mass} (resembling $Q_{P\ seismic}$ if in GPa), and to the stress-dependent P-wave velocity V_P (see Barton, 2006, 2007c).

References

Bakhtar, K. & Barton, N. Large scale static and dynamic friction experiments. *Proc. 25th US Rock Mechanics Symp.* Northwestern Univ., Illinois. 1984.

Bandis, S., Lumsden, A. & Barton, N. Experimental studies of scale effects on the shear behaviour of rock joints. *Int. J. of Rock Mech. Min. Sci. and Geomech. Abstr*. 18, 1-21, 1981.

Bandis, S., Lumsden, A.C. & Barton, N. Fundamentals of rock joint deformation. *Int. J. Rock Mech. Min. Sci. and Geomech. Abstr.* 20, 249-268, 1983.

Barton, C.A., Zoback, M.D. & Moos, D. In situ stress and permeability in fractured and faulted crystalline rock. *Mechanics of Jointed and Faulted Rock.*, Rossmanith (Ed.). 381–396. Rotterdam: Balkema, 1995.

Barton, N. A model study of air transport from underground openings situated below groundwater level. Proc. of Symp. of Int. Soc. Rock Mech., *Percolation through fissured rock*, Stuttgart, Theme 3A, 20, 1972.

Barton, N. Review of a new shear strength criterion for rock joints, *Engineering Geology*, Elsevier, Amsterdam, Vol. 7, 287-332, 1973.

Barton, N. The shear strength of rock and rock joints. I*nt. Jour. Rock Mech. Min. Sci. and Geomech. Abstr*., Vol. 13, No. 9: 255-279, 1976.

Barton, N. & Choubey, V. The shear strength of rock joints in theory and practice. *Rock Mechanics* 1/2:1-54. Vienna: Springer,1977.

Barton, N. Hydraulic fracturing to estimate minimum stress and rockmass stability at a pumped hydro project. Proc. of *Workshop on Hydraulic Fracturing Stress Measurements*, Monterey, California, 1981.

Barton, N. Modelling rock joint behaviour from in situ block tests: Implications for nuclear waste repository design. *Office of Nuclear Waste Isolation*, Columbus, OH, 96 p., ONWI-308, September 1982.

Barton, N. and Bakhtar, K. TerraTek contract report for AECL, Canada later published in two volumes by CANMET. Description and modelling of rock joints for the hydrothermalmechanical design of nuclear waste vaults. Atomic Energy of Canada Limited. TR-418. Volumes I and II. 1983, 1987.

Barton, N., Bandis, S. & Bakhtar, K. Strength, deformation and conductivity coupling of rock joints. *Int. J. Rock Mech. & Min. Sci. & Geomech. Abstr*. 22: 3: 121-140, 1985.

Barton, N. Deformation phenomena in jointed rock. 8th Laurits Bjerrum Memorial Lecture, Oslo. *Geotechnique*, London, Vol. 36: 2: 147-167, 1986.

Barton, N., Hårvik, L., Christiansson, M., Bandis, S., Makurat, A., Chryssanthakis, P. & Vik, G. Rock mechanics modelling of the Ekofisk reservoir subsidence. Proc. 27th US Rock Mech. Symp., Univ. of Alabama, 1986.

Barton, N., Makurat, A., Hårvik, L., Vik, G., Bandis, S., Christianson, M. & Addis, A. The discontinuum approach to compaction and subsidence modelling as applied to Ekofisk. *BOSS '88. Proc. of Int. Conf. on Behaviour of Offshore Structures*, Trondheim. Vol. 1: 129-141, 1988.

Barton, N. and Quadros, E.F. Joint aperture and roughness in the prediction of flow and groutability of rock masses. Proc. of NY Rocks '97. Linking Science to Rock Engineering. Ed. K. Kim, 907-916. *Int. J. Rock Mech. and Min. Sci*. Vol. 34: No. 3-4, 1997.

Barton, N. General report concerning some 20th Century lessons and 21st Century challenges in applied rock mechanics, safety and control of the environment. *Proc. of 9th ISRM Congress*, Paris, 3: 1659-1679, Balkema, Netherlands, 1999.

Barton, N. *Rock Quality, Seismic Velocity, Attenuation and Anisotropy.* Taylor & Francis, UK & Netherlands, 729 p, 2006.

Barton, N. Anisotropy and 4D caused by two fracture sets, four compliances, and sheared apertures. *The Leading Edge, SEG*, Sept. 2007, 1112-1117, 2007a.

Barton, N. Near-surface gradients of rock quality, deformation modulus, Vp and Qp to 1km depth. First Break, *EAGE*,October, 2007, Vol. 25, 53-60, 2007b.

Barton, N. Geomechanics and geophysical processes in naturally fractured reservoirs. *2nd. EAGE Workshop on Naturally Fractured Reservoirs*, Muscat, Oman, 33-37, 2013a.

Barton, N. Characterization of fracture shearing for 4D interpretation of fractured reservoirs. *2nd. EAGE Workshop on Naturally Fractured Reservoirs*, Muscat, Oman, 72-76, 2013b.

Barton, N. The shear strength of rock, rock joints, and rock masses: problems and some solutions. *Eurock,*, Vigo, Spain. Keynote lecture, 15p, 2014a.

Barton, N. Non-linear behaviour for naturally fractured carbonates and frac-stimulated gas shales. First Break, Vol. 32, 51-66, Sept. 2014b.

Barton, N. and E. Quadros. Gas-shale fracturing and fracture mobilization in shear: *Quo Vadis*? *Rock Mechanics for Natural Resources and Infrastructure. SBMR.* ISRM Speciality Conference, Goiania, Brazil, 12p.

Barton, N. and E. Quadros. Anisotropy is everywhere, to see, to measure and to model. Rock Mechanics and Rock Engineering, Rock Mechanics and Rock Engineering. July 2015, Volume 48, pp 1323-1339, 2015.

Byerlee, James D. Friction of Rocks. *Pure and Applied Geophysics* 116 (4-5): 615–626, 1978.

Chryssanthakis, P., Monsen, K. & Barton, N. Validation of UDEC-BB against the CSM block test and large scale application to glacier loading of jointed rock masses. *Proc. 7th ISRM Cong.*, Aachen. 693–698, 1991.

Dusseault, M. Geomechanical aspects of shale gas development. Keynote lecture, Eurock2013, Wroclow, Poland. *Rock Mechanics for Resources, Energy and Environment. Kwasniewski & Lydzba.* Taylor and Francis, London, p. 39-56, 2013.

Fairhurst, C. Fractures and Fracturing: Hydraulic Fracturing in Jointed Rock. Proc. of Int. Conf. *Effective and Sustainable Hydraulic Fracturing*. An ISRM specialized Conference, Bunger, McLennan, and Jeffrey (editors). Chapter 3, Brisbane, Australia, May 2013.

Fisher, K. and N. Warpinski. Hydraulic Fracture-Height Growth: Real Data *SPE Annual Technical Conference*, Denver, Colorado, USA. SPE 145949, 18p, 2011.

Ghassemi, A. and R. Suarez-Rivera. Sustaining fracture area and conductivity of gas shale reservoirs for enhancing long-term productivity and recovery. RPSEA, (Research Partnership to Secure Energy for America). Final report, 08122-48, 253p, 2012.

Gutierrez, M., Oino, L., and Nygard, R. Stress-dependent permeability of a demineralised fracture in shale, *Marine and Petroleum Geology*, **17(8)**, p. 895-907, 2000.

Gentier, S.D. Comportement hydro-mécanique d'une fracture naturelle sous contrainte normale. *Proc. of 6th ISRM Cong. On Rock Mech*., Montréal, Canada, pp. 105-108, 1987.

Han, G. Natural fractures in unconventional reservoir rocks: identification, characterization, and its impact to engineering design. Proc. 45th US Rock Mechanics/Geomechanics Symp., San Fransisco, USA, 2011.

King, G. Thirty years of gas shale fracturing: what we have learned? SPE 133456. *The SPE Annual Technical Conference and Exhibition, 19-22 September 2010*. Florence, Italy, 2010.

Makurat, A., Barton, N., Rad, N.S. & Bandis, S. Joint conductivity variation due to normal and shear deformation. *Int. Symp. on Rock Joints.* Loen 1990. Balkema, 535-540, 1990.

Makurat, A. & Barton, N. Rock mechanical computation of deformations and joint apertures during excavation of the Fjellinjen tunnels. Paper 27.1-27.27, *Bergmekanikkdag*, Tapir Press, Oslo, 1988.

Nagel, N.B., M. A. Sanchez-Nagel, F. Zhang, X. Garcia & B. Lee. Coupled numerical evaluations of the geomechanical interactions between a hydraulic fracture stimulation and a natural fracture system in shale formations. *Rock Mechanics and Rock Engineering,* Vol. 46, No. 3, 581-609, 2013.

Olsson, R. and N. Barton. An improved model for hydro-mechanical coupling during shearing of rock joints. *Int. J. Rock Mech.& Min. Sci.* 38: 317-329. Pergamon, 2001.

Pine, R.J. and A.S. Bachelor. Downward migration of shearing in jointed rock during hydraulic injections. *Int. J. Rock Mech. & Min. Sci. Geomech. Abstr.* 21, 5: 249-263, 1984.

Singh, M., Raj, A. and B. Singh. Modified Mohr-Coulomb criterion for non-linear triaxial and polyaxial strength of intact rocks. *Int. J. Rock Mech. Mining Sci.,* 48(4), 546-555, 2011.

Warpinski, N., J.Du and U.Zimmer. Measurements of hydraulic-fracture-induced seismicity in gas shales. SPE 151597. SPE Hydraulic Fracturing Technology Conference, Texas, USA, 2012.

Zoback, M., S.Kitasei and B. Copithorne. Addressing the environmental risks from shale gas development. Worldwatch Institute, *Natural Gas and Sustainable Energy Initiative*. Briefing P1, 1-18, 2010.

Zoback, M.D. & Townend, J. Implications of hydrostatic pore pressures and high crustal strength for the deformation of intraplate lithosphere. *Tectonophysics*, *336*: 19–30, 2001.

Zoback, M.D. *Reservoir Geomechanics.* Cambridge University Press, 449p, 2007.